


Localized nonlinear waves and dynamical stability in spinor Bose–Einstein condensates with time–space modulation

Yu-Qin Yao¹ , Wei Han², Ji Li³ and Wu-Ming Liu³

¹Department of Applied Mathematics, China Agricultural University, Beijing 100083, People's Republic of China

²Key Laboratory of Time and Frequency Primary Standards, National Time Service Center, Chinese Academy of Sciences, Xian 710600, People's Republic of China

³Beijing National Laboratory for Condensed Matter Physics, Institute of Physics, Chinese Academy of Sciences, Beijing 100190, People's Republic of China

E-mail: yyqinw@126.com

Received 21 July 2017, revised 22 March 2018

Accepted for publication 5 April 2018

Published 25 April 2018



Abstract

Nonlinearity is one of the most remarkable characteristics of Bose–Einstein condensates (BECs). Much work has been done on one- and two-component BECs with time- or space-modulated nonlinearities, while there is little work on spinor BECs with space–time-modulated nonlinearities. In the present paper we investigate localized nonlinear waves and dynamical stability in spinor Bose–Einstein condensates with nonlinearities dependent on time and space. We solve the three coupled Gross–Pitaevskii equations by similarity transformation and obtain two families of exact matter wave solutions in terms of Jacobi elliptic functions and the Mathieu equation. The localized states of the spinor matter wave describe the dynamics of vector breathing solitons, moving breathing solitons, quasi-breathing solitons and resonant solitons. The results show that one-order vector breathing solitons, quasi-breathing solitons, resonant solitons and the moving breathing solitons $\psi_{\pm 1}$ are all stable, but the moving breathing soliton ψ_0 is unstable. We also present the experimental parameters to realize these phenomena in future experiments.

Keywords: spinor Bose–Einstein condensates, time–space modulation, localized nonlinear waves, dynamical stability

(Some figures may appear in colour only in the online journal)

1. Introduction

For a decade experimental realization of Bose–Einstein condensates (BECs) at ultra-low temperatures has attracted much interest from atomic physicists [1, 2]. In recent years, one of the most important developments in BECs has been the study of spinor condensates. The idea of spinor condensates was proposed by Ho and Ohmi [3, 4]. Stamper-Kurn *et al* created spinor condensates experimentally [5], providing a new way to observe phenomena that are not present in single-component BECs. These

include the formation of spin domains and spin textures [6, 7]. In contrast to single- and two-component BECs, the spin- F condensates described by macroscopic wave functions with $2F+1$ components have some new characteristics, including the vector character of the order parameter and the changed role of spin relaxation collisions. Very many studies have been done and it is now a hot research topic. For example, in 2014, Kanna investigated the dynamics of bright matter wave solitons in spin-1 Bose–Einstein condensates with time-modulated nonlinearities and obtained soliton solutions of an integrable

autonomous three coupled GP equation (GPE) [8]. Liu derived exact static as well as moving solitonic solutions to the one-dimensional spin-orbit-coupled $F = 1$ BECs [9]. In 2015, Seo researched the half-quantum vortices (HQVs) in the easy-plane polar phase of antiferromagnetic spinor BECs and performed a collision experiment with two HQV pairs [10, 11]. In 2016, Oshima studied the spin Hall effect in a spinor dipolar BECs and discussed a possible experimental situation [12]. Ollikainen studied the density profiles, phase profiles and angular momentum in the spin-1 system [13]. Recently, the internal structure and stability of vortices in a dipolar spinor BEC and vortex-bright solitons in a spin-orbit-coupled spin-1 condensate have been studied [14, 15]. However, there has so far been little work on spinor BECs with time-space-modulated nonlinearity.

Matter waves, as the natural outcomes of mean-field descriptions, have been observed experimentally and investigated theoretically [16–18]. For example, matter wave solitons could be used for applications in optical lattices, atomic lasers, atomic interferometry and coherent atom transport. Moreover, matter wave solitons are also helpful for the realization of quantum information processing and computation [19, 20]. So it would be interesting to develop a new technique for constructing particular solitons. One possible technique is to alter the interatomic interactions by means of Feshbach resonance [21, 22]. Temporal nonlinearity modulation can create bright solitons, induce collapse, and so on [23–25]. Spatial nonlinearity modulation can support persistent Bloch oscillations and may break the stability limit imposed by the Vakhitov–Kolokolov criterion [26, 27]. This led to a good proposal for manipulation of nonlinear excitations and matter waves by controlling the time-dependent or space-dependent scattering strength. In the past decades, several types of Feshbach resonance, for example magnetic Feshbach resonance [28, 29], optical Feshbach resonance [30, 31], confinement-induced resonance [32, 33] and orbital Feshbach resonance [34, 35], have been successively developed and have proved to be extremely useful tools for tailoring the interaction.

In the conventional case, the interaction is changed independently of time and space [21, 22, 28–35]. However, some kinds of interactions with simple spatial [36, 37] or time modulation [38–41] have also been theoretically suggested and experimentally realized. For example, submicron spatial control of the scattering length has been experimentally realized in a ytterbium BEC by a pulsed optical standing wave near an optical Feshbach resonance [36], which proves that high-resolution control of atomic interactions is possible. Square-waveform time modulation of the scattering length has also been theoretically proposed [38] and experimentally realized [39] in rubidium condensates using a carefully controlled magnetic field pulse. In addition, there is also a relevant breakthrough towards the realization of interaction with both

time and space modulation in [42], where high speed and spatially resolved control of interaction has been achieved in a stable BEC of cesium atoms by optical control of Feshbach resonances. All these developments indicate that it may be possible to implement interactions with both time and space modulation in the future, and provide support for research into time-space-modulated nonlinearity.

In this paper we consider spinor BECs with space- and time-dependent nonlinearities, which can be described by the three-component GPE. Unlike with one- and two-component BECs, we can use an optically induced Feshbach resonance [43] or a confinement-induced resonance [44] to tune the nonlinearities in spinor BECs. Two families of localized nonlinear matter waves are given based on the Mathieu equation and Jacobi elliptic function, which take the form of vector solitons. We investigate in detail vector breathing solitons, moving breathing solitons, quasi-breathing solitons and resonant solitons. The dynamical stability of vector solitons is studied by means of numerical simulations and the global stability of the different types of vector solitons is analyzed. The results show that one-order vector breathing solitons, quasi-breathing solitons, resonant solitons and the moving breathing solitons $\psi_{\pm 1}$ are all stable but the moving breathing soliton ψ_0 is unstable.

2. Localized nonlinear matter wave solutions

Here we focus on BECs of alkali atoms (^{23}Na) in the $F = 1$ hyperfine state [6], confined in the trapping potential $V_{ext} = \frac{m}{2}(\omega_x^2 x^2 + \omega_{\perp}^2(y^2 + z^2))$ with m the mass of atoms and ω_x and ω_{\perp} the confining frequencies in axial and radial directions. Under the mean-field approximation, the dynamics of the spinor condensates can be described by a three-component GPE in three dimensions. When the longitudinal trap frequency ω_x is much less than the transverse one ω_{\perp} , the three-dimensional GPE can be reduced to a one-dimensional equation, which can be realized experimentally with the apparatus described in [45].

In the absence of an external magnetic field, the three internal states $m_F = 1, 0, -1$, with m_F the magnetic quantum number, are generated, in which an $m_F = 1$ and an $m_F = -1$ atom can collide and produce two $m_F = 0$ atoms, and vice versa. The spin-1 BECs can be described by the vectorial wave function $\Psi(x, t) = (\psi_1(x, t), \psi_0(x, t), \psi_{-1}(x, t))^T$ with the components corresponding to the three values of the vertical spin projection $m_F = 1, 0, -1$. When the temperature is lower than the critical temperature, the wave functions are governed by a set of three coupled

dimensionless GPEs [3, 46]:

$$\begin{aligned}
 i\frac{\partial\psi_1}{\partial t} &= \left(-\frac{\nabla^2}{2} + g_n(|\psi_1|^2 + |\psi_0|^2 + |\psi_{-1}|^2) \right. \\
 &\quad \left. + g_s(|\psi_1|^2 + |\psi_0|^2 - |\psi_{-1}|^2) + V + E_1\right)\psi_1 \\
 &\quad + g_s\psi_{-1}\psi_0^2, \\
 i\frac{\partial\psi_0}{\partial t} &= \left(-\frac{\nabla^2}{2} + g_n(|\psi_1|^2 + |\psi_0|^2 + |\psi_{-1}|^2) \right. \\
 &\quad \left. + g_s(|\psi_1|^2 + |\psi_{-1}|^2) + V + E_0\right)\psi_0 + 2g_s\psi_{-1}\psi_0^*\psi_1, \\
 i\frac{\partial\psi_{-1}}{\partial t} &= \left(-\frac{\nabla^2}{2} + g_n(|\psi_1|^2 + |\psi_0|^2 + |\psi_{-1}|^2) \right. \\
 &\quad \left. + g_s(|\psi_{-1}|^2 + |\psi_0|^2 - |\psi_1|^2) \right. \\
 &\quad \left. + V + E_{-1}\right)\psi_{-1} + g_s\psi_1^*\psi_0^2.
 \end{aligned} \tag{1}$$

Here, $\nabla^2 = \frac{\partial^2}{\partial x^2}$, $V = \frac{\omega^2 x^2}{2}$ is a one-dimensional trapping potential and $\omega = \frac{\omega_x}{\omega_\perp}$ is the trap's aspect ratio. $E_j \in \mathbb{R}$ is the dimensionless Zeeman energy of spin components $m_F = -1, 0, 1$ and $|\psi_1|^2 + |\psi_0|^2 + |\psi_{-1}|^2$ is the total condensate density. The strength of the interaction is given by $g_n = \frac{4\pi\hbar^2(a_0 + 2a_2)}{3m}$, $g_s = \frac{4\pi\hbar^2(a_2 - a_0)}{3m}$, where \hbar is the reduced Planck constant and a_0 and a_2 are the s-wave scattering lengths of the scattering channel of total hyperfine spin-0 and spin-2, respectively [47]. The length and time are measured in units of $\sqrt{\frac{\hbar}{m\omega_\perp}}$ and ω_\perp^{-1} , respectively. Here we provide the experimental parameters for producing a spinor condensate composed of ^{23}Na [48, 49] with the total number $N = 3 \times 10^6$. The external trapping potential is given by $V = \frac{\omega^2 x^2}{2}$ with $\omega = 2\pi \times 230$ Hz. The scattering lengths are $a_0 = 50a_B$ and $a_2 = 55a_B$ with Bohr radius $a_B = 0.529 \text{ \AA}$. In our case, the trapping potential is taken as $V = \frac{(\omega_0^2 + \epsilon \cos(\bar{\omega}t))x^2}{2}$ ($\epsilon \in (-1, 1)$, $\omega_0, \bar{\omega} \in \mathbb{R}$) modulated by time t , and the scattering lengths are taken as $g_n = c_n \lambda(t)^{-\frac{3}{2}} e^{-\frac{3(\lambda(t)x + \delta(t))^2}{2}}$, $g_s = c_s \lambda(t)^{-\frac{3}{2}} e^{-\frac{3(\lambda(t)x + \delta(t))^2}{2}}$ (c_n and c_s are constants) depending on time and space, which can be realized by controlling the induced Feshbach resonances optically induced or confinement-induced resonances in the real BEC experiments.

In the following we seek the exact localized solutions of (1) for $\lim_{|x| \rightarrow \infty} \psi_{\pm 1,0} = 0$. To do this, the similarity transformations

$$\begin{aligned}
 \Psi_1 &= \beta_1(x, t)U(X(x, t))e^{i\alpha_1(x, t)}, \\
 \Psi_{-1} &= \beta_{-1}(x, t)R(X(x, t))e^{i\alpha_{-1}(x, t)}, \\
 \Psi_0 &= \beta_0(x, t)W(X(x, t))e^{i\frac{\alpha_1(x, t) + \alpha_{-1}(x, t)}{2}},
 \end{aligned} \tag{2}$$

are taken to transform (1) to the ordinary differential equations (ODEs)

$$\begin{aligned}
 U_{XX} + b_{11}U^3 + b_{12}UR^2 + b_{13}W^2U &= 0, \\
 R_{XX} + b_{21}U^2R + b_{22}R^3 + b_{23}W^2R &= 0, \\
 W_{XX} + b_{31}R^2W + b_{32}U^2W + b_{33}W^3 + b_{34}URW &= 0,
 \end{aligned} \tag{3}$$

and the partial differential equations (PDEs)

$$\begin{aligned}
 \frac{1}{2}\beta_{1xx} - \beta_1\alpha_{1t} - (V + E_1)\beta_1 &= 0, \\
 \beta_{i,x}X_x + \frac{1}{2}\beta_i X_{xx} &= 0, \quad (i = 0, \pm 1) \\
 \beta_{it} + \beta_i\alpha_{ix} + \frac{1}{2}\beta_i\alpha_{ixx} &= 0, \quad (i = \pm 1) \\
 X_t + \alpha_{ix}X_x &= 0, \quad (i = \pm 1), \\
 \frac{1}{2}\beta_{-1,xx} - \beta_{-1}\alpha_{-1,t} - (V + E_2)\beta_{-1} &= 0 \\
 \frac{1}{2}\beta_0(\alpha_{1t} + \alpha_{2t} + \frac{1}{4}\alpha_{1x}^2 + \frac{1}{4}\alpha_{2x}^2) + \frac{1}{2}\beta_{0xx} \\
 - \frac{1}{4}\beta_0\alpha_{1x}\alpha_{2,x} - (V + E_0)\beta_0 &= 0, \\
 \frac{1}{2}\beta_{0x}(\alpha_{1x} + \alpha_{2x}) + \beta_{0t} + \frac{1}{4}\beta_0(\alpha_{1xx} + \alpha_{2xx}) &= 0
 \end{aligned} \tag{4}$$

where b_{ij} ($i = 1, 2, 3$ and $j = 1, 2, 3, 4$) are constants. To obtain explicit solutions, we choose ω^2 in the form

$$\omega^2 = \omega_0^2 + \epsilon \cos(\bar{\omega}t) \tag{5}$$

and take $X = \frac{1}{2}\sqrt{\pi} \operatorname{erf}(\lambda(t)x + \delta(t))$, where $\operatorname{erf}(s) = \frac{2}{\sqrt{\pi}} \int_0^s e^{-\tau^2} d\tau$ is called an error function and $\epsilon \in (-1, 1)$ and $\omega_0, \bar{\omega} \in \mathbb{R}$. The trapping potential plays a critical role in adjusting the amplitude, phase and propagation velocity, while the localization of the predicted soliton solutions does not depend on it. The localized solutions exist even when the trapping potential is very small with the trapping frequency $\omega \sim 0$.

Now under the condition $E_1 + E_{-1} = E_0$, solving the PDEs (4) gives

$$\begin{aligned}
 \alpha_{\pm 1}(x, t) &= -\frac{\lambda(t)_t x^2 + 2\delta(t)_t x}{2\lambda(t)} + \xi_{\pm 1}(t), \quad \beta_j(x, t) \\
 &= c_j \lambda(t)^{\frac{1}{2}} e^{\frac{\lambda(t)x + \delta(t)}{2}},
 \end{aligned} \tag{6}$$

with

$$\begin{aligned}
 \lambda(t) &= \left(A \sin^2 \omega t + B \cos^2 \omega t \right. \\
 &\quad \left. + \frac{2\sqrt{\omega^2(AB\omega^2 - 1)} \sin \omega t \cos \omega t}{\omega^2} \right)^{-\frac{1}{2}}, \\
 \xi(t)_{\pm 1} &= \frac{1}{2} \int \frac{\lambda^4 + \lambda^4 \delta^2 - \delta_t^2}{\lambda^2} dt - E_{\pm 1} t, \\
 \delta(t) &= c_2 e^i \int \lambda^2 dt + c_3 e^{-i} \int \lambda^2 dt,
 \end{aligned} \tag{7}$$

where c_j ($j = -1, 0, 1, 2, 3$) are arbitrary constants and A, B and C are constants satisfying $AB - C^2 = \frac{1}{\xi_1 \xi_2 - \xi_2 \xi_1}$ with (ξ_1, ξ_2) being two linear independent solutions of the Mathieu equation [50, 51]

$$\xi_{tt} + \omega^2 \xi = 0. \tag{8}$$

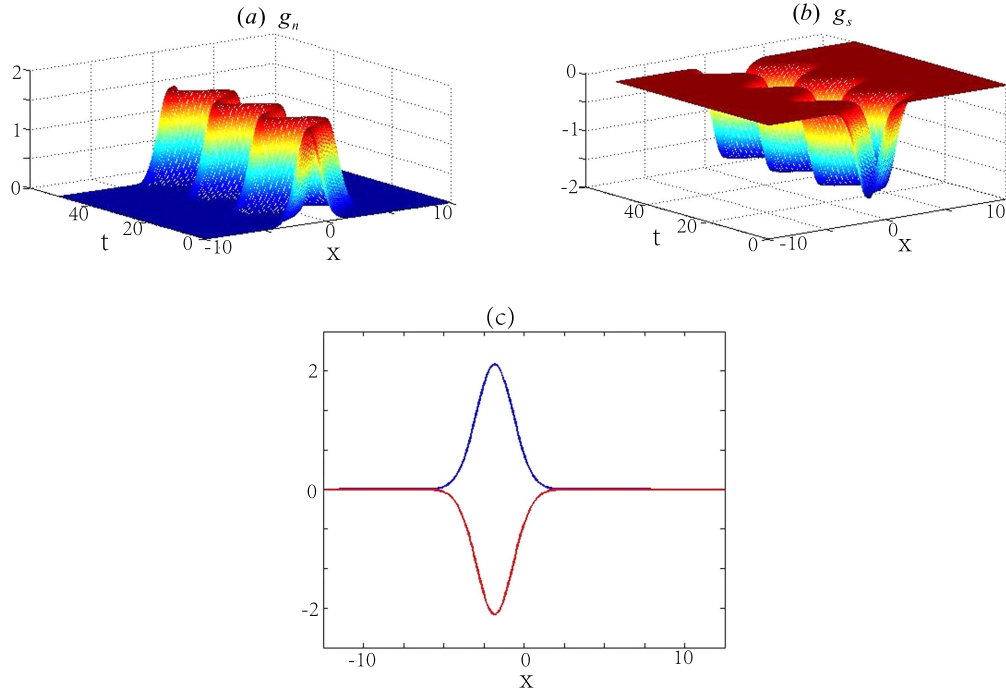


Figure 1. Parts (a) and (b) show examples of spatiotemporal-dependent nonlinearities g_n and g_s with $\omega = 0.4$, respectively. (c) Nonlinearities g_n (red) and g_s (blue) for $t = 1$ and $\omega = 0.4$, respectively. It can be seen that g_n and g_s are space-localized and time-periodic.

Solving the ODEs (3), we obtain two families of exact solutions

$$\begin{aligned} U^{(1)} &= -C_s \operatorname{cn}\left(\mu_1 X, \frac{\sqrt{2}}{2}\right), \\ V^{(1)} &= C_s \operatorname{cn}\left(\mu_1 X, \frac{\sqrt{2}}{2}\right), \\ W^{(1)} &= \operatorname{cn}\left(\mu_1 X, \frac{\sqrt{2}}{2}\right), \end{aligned} \quad (9)$$

and

$$\begin{aligned} U^{(2)} &= -C_s \operatorname{sd}\left(\mu_2 X, \frac{\sqrt{2}}{2}\right), \\ V^{(2)} &= C_s \operatorname{sd}\left(\mu_2 X, \frac{\sqrt{2}}{2}\right), \\ W^{(2)} &= \operatorname{sd}\left(\mu_2 X, \frac{\sqrt{2}}{2}\right). \end{aligned} \quad (10)$$

Here, $C_s = \sqrt{\frac{-c_0^2 b_{12} + 2c_1^2 \mu_1^2}{2c_1^2 b_{12}}}$, μ_1 and μ_2 are arbitrary constants and cn and $\operatorname{sd} = \operatorname{sn}/\operatorname{dn}$ are Jacobi elliptic functions. The solutions (9) and (10) exist for any ratio of the density–density and spin-exchange interactions with $g_n = a g_s$, where a is an arbitrary constant. In the following, we discuss the case with interaction parameters satisfying $g_n = -g_s$ as an example. When imposing the bounded condition $\lim_{|x| \rightarrow \infty} \psi_{\pm 1,0}(x) = 0$, we have $\mu_1 = \frac{2(2n+1)K(\frac{\sqrt{2}}{2})}{\sqrt{\pi}}$ and $\mu_2 = \frac{4mK(\frac{\sqrt{2}}{2})}{\sqrt{\pi}}$, where the natural numbers n and m are the orders of the solitons, and $K(\frac{\sqrt{2}}{2}) = \int_0^{\pi/2} \left[1 - \frac{1}{2} \sin^2 \xi\right]^{-\frac{1}{2}} d\xi$.

Based on (6) and (7)–(10), we work out two families of exact solutions of the dimensionless GPE (1)

$$\begin{aligned} \psi_1^{(j)} &= c_1 \sqrt{\lambda(t)} e^{\frac{\delta(t)^2}{2}} e^{\gamma(x,t) + i\alpha_1(x,t)} U^{(j)}(X), \\ \psi_{-1}^{(j)} &= c_{-1} \sqrt{\lambda(t)} e^{\frac{\delta(t)^2}{2}} e^{\gamma(x,t) + i\alpha_{-1}(x,t)} R^{(j)}(X), \\ \psi_0^{(j)} &= c_0 \sqrt{\lambda(t)} e^{\frac{\delta(t)^2}{2}} e^{\gamma(x,t) + \frac{i(\alpha_1(x,t) + \alpha_{-1}(x,t))}{2}} W^{(j)}(X), \end{aligned} \quad (11)$$

where $\delta(t)$, $\alpha_{\pm 1}(x, t)$ are given in (7), and $U^{(j)}$, $R^{(j)}$, $W^{(j)}$ ($j = 1, 2$) are given in (9)–(10). The significance of each quantity is as follows: $\gamma(x, t) = \lambda(t) x(\lambda(t) x + 2\delta(t))$ is the coordinate for observing the soliton’s envelope; $\alpha_1(x, t)$ is the coordinate for observing the soliton’s carrier waves; $\sqrt{\lambda(t)} e^{\frac{\delta(t)^2}{2}}$ is the amplitude of the solitons. It is easy to see that $\lim_{|x| \rightarrow \infty} \psi_{\pm 1,0}(x) = 0$ by direct computation, so these two families of solutions are localized nonlinear wave solutions.

3. Dynamics of the localized nonlinear matter wave

We now discuss how the spatiotemporal-dependent nonlinearities g_n and g_s control the dynamics of the localized matter waves given by (11). In the special case, the expressions of g_n and g_s can be simplified. In the case of parameters $A = B = \frac{1}{\omega}$ and $c_2 = c_3 = 0$ the nonlinearities become $g_n = \frac{c_n}{4\sqrt{\omega^3}} e^{-\frac{3\omega x^2}{2}}$ and $g_s = \frac{c_s}{4\sqrt{\omega^3}} e^{-\frac{3\omega x^2}{2}}$, which are space-localized Gaussian nonlinearities. In the case of parameters $A = B = \frac{1}{\omega}$ and $c_2 = c_3 = \frac{1}{2}$, the nonlinearities become $g_n = \frac{c_n}{4\sqrt{\omega^3}} e^{-\frac{3(\sqrt{\omega x} + \cos \omega t)^2}{2}}$ and $g_s = \frac{c_s}{4\sqrt{\omega^3}} e^{-\frac{3(\sqrt{\omega x} + \cos \omega t)^2}{2}}$, which are time-periodic localized nonlinearities as shown in figure 1. In

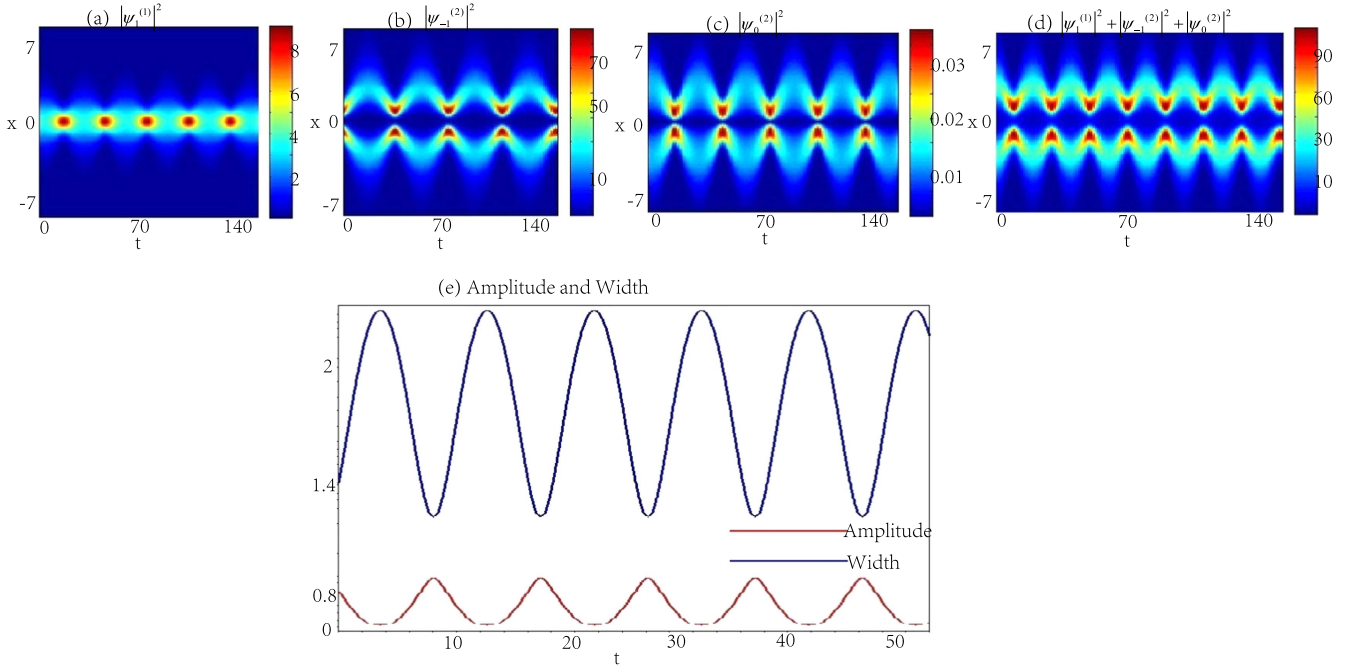


Figure 2. Dynamics of the breathing solitons in a spin-1 BEC with spatiotemporally modulated nonlinearities. Parts (a) to (d) exhibit the evolution of the density distribution $|\psi_1^{(1)}|^2$, $|\psi_{-1}^{(2)}|^2$, $|\psi_0^{(2)}|^2$ and the total density distribution $|\psi_1^{(1)}|^2 + |\psi_{-1}^{(2)}|^2 + |\psi_0^{(2)}|^2$, respectively. Part (e) illustrates the amplitude (red) and width (blue) of the wave functions. The ratio of the confining frequency is taken as $\omega = 0.4$.

real BEC experiments they can be generated by the optically induced Feshbach resonances or confinement-induced resonances.

The management of spatiotemporal nonlinearities can generate solitons with novel properties. According to different choices of $\bar{\omega}$ and ϵ , different types of behaviors can be classified as:

- (a) breathing solitons, when $\epsilon = 0$,
- (b) quasi-periodic solitons, when $\epsilon \neq 0$ and the two linear independent solutions ξ_1 and ξ_2 belong to the stability domain of (8),
- (c) resonant solitons, when $\epsilon \neq 0$ and ξ_1 and ξ_2 are in the instability domain of (8).

In this section we will consider the dynamics of localized nonlinear matter waves and propose how to control them by the external trapping potential and space-time inhomogeneous s-wave scattering lengths in future experiments. In the following, we take a ^{23}Na condensate containing 3×10^6 atoms and the parameters are taken as $c_{-1} = 1$, $c_0 = 0.5$, $c_1 = 1$, $b_{12} = 0.5$, $A = 5$ and $B = 2$.

3.1. Breathing solitons

Here, we take $\epsilon = 0$. In this case, the trapping potential $V = \frac{\omega_0^2 x^2}{2}$ and the interactions $g_n = -g_s = -\frac{b_{12}}{4c_{-1}^2 \lambda(t)} e^{-(\lambda(t)x + \delta(t))^2}$ are all space- and time-dependent, and can be realized by controlling the optically induced Feshbach resonance or a confinement-induced resonance in real BEC experiments. The

corresponding localized nonlinear wave can be obtained from (11). These solutions show different features according to the choice of the parameter $\delta(t)$. The ratio of the confining frequency $\omega = 0.4$. In figure 2, we show the evolution of density profiles for the one-order wave functions $\psi_1^{(1)}$ and $\psi_{-1,0}^{(2)}$ with the above parameters. The density profiles for $\psi_1^{(1)}$ and $\psi_{-1,0}^{(2)}$ are the same as for $\psi_1^{(1)}$ and $\psi_{-1,0}^{(2)}$. It can be observed that the density wave packets are localized in space and oscillate periodically in time, and are called breathing solitons. Here $\sqrt{\lambda(t)}$ and $1/\lambda(t)$ are the amplitude and width of the matter wave, respectively. Figures 2(a) to (c) describe the density profiles of the one-order wave functions $\psi_1^{(1)}$, $\psi_{-1}^{(2)}$ and $\psi_0^{(2)}$, respectively. Figure 2(d) shows the total density distribution $|\psi_1^{(1)}|^2 + |\psi_{-1}^{(2)}|^2 + |\psi_0^{(2)}|^2$ for the spinor BECs. Figure 2(e) illustrates the amplitude $\sqrt{\lambda(t)}$ and width $1/\lambda(t)$ of the wave functions. It is observed that the amplitude and width of the localized nonlinear waves vary periodically with increasing time. In all the figures in this paper the units of space length and time are $1.38 \mu\text{m}$ and 0.7ms .

When $\delta(t) \neq 0$ and $\delta(t)$ is given by (7). In this situation, the trapping potential is still time-independent, but the interactions g_n and g_s given by (6) and (7) become more complex, so the amplitude of the nonlinear matter wave becomes $\sqrt{\lambda(t)} e^{\frac{\delta(t)^2}{2}}$ and the center of mass of the solitons moves time periodically with non-zero velocity. So the nonlinear matter waves are called moving breathing. For convenience, we assume the ratio of the confining frequencies ω is time-independent to illustrate the dynamics of a moving

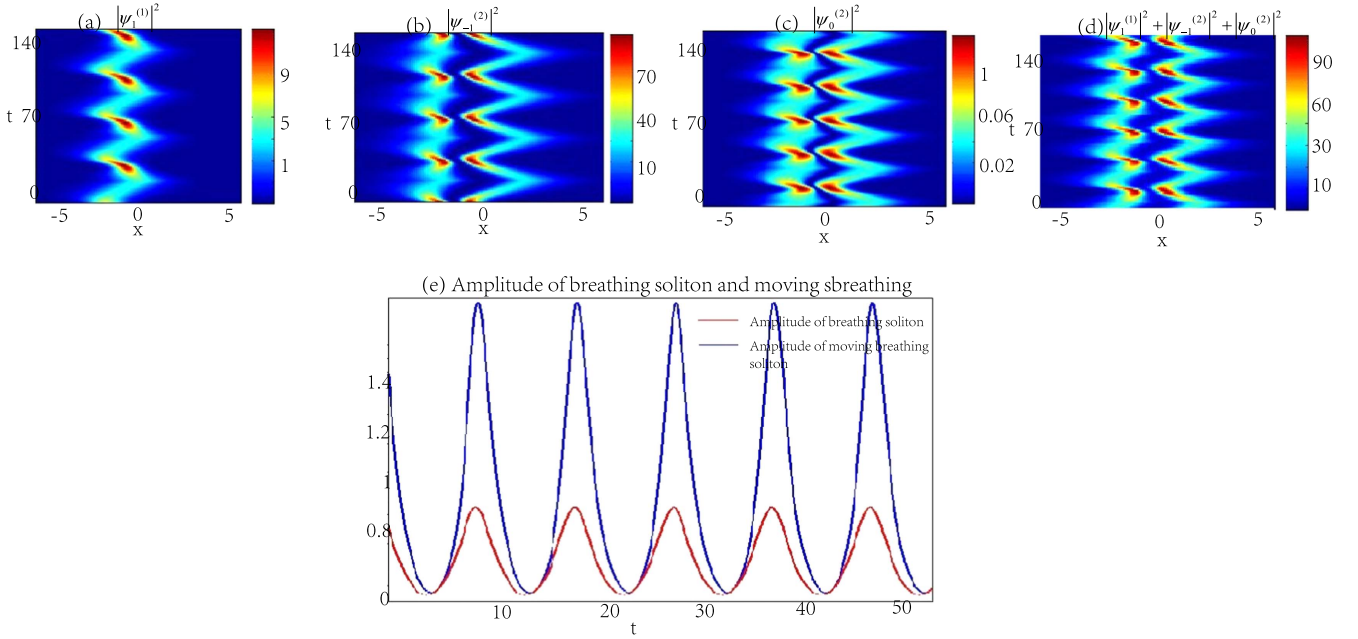


Figure 3. Dynamics of the moving breathing solitons in a spin-1 BEC with spatiotemporally modulated nonlinearities. Parts (a) to (d) show the time evolution of the density distributions $|\psi_1^{(1)}|^2$, $|\psi_{-1}^{(2)}|^2$, $|\psi_0^{(2)}|^2$ and $|\psi_1^{(1)}|^2 + |\psi_{-1}^{(2)}|^2 + |\psi_0^{(2)}|^2$, respectively. Parts (e) shows the amplitude of the breathing solitons (red) and the moving breathing solitons (blue). The ratio of the confining frequency is still taken as $\omega = 0.4$ and the other parameters are taken as $c_2 = c_3 = 1/3$.

breathing soliton. Here we still take $\omega = 0.4$ and $\epsilon = 0$. Figures 3(a)–(c) describe the time evolution of the density profiles of one-order wave functions $\psi_1^{(1)}$, $\psi_{-1}^{(2)}$ and $\psi_0^{(2)}$, respectively. Figure 3(d) illustrates the total density distribution $|\psi_1^{(1)}|^2 + |\psi_{-1}^{(2)}|^2 + |\psi_0^{(2)}|^2$ for the spinor BECs. It can be observed the nonlinear matter waves are space-localized and move periodically with respect to time. Figure 3(e) describes the amplitude of the breathing solitons (red) and moving breathing solitons (blue). It can be seen that the amplitudes of the nonlinear waves vary periodically versus t , and the amplitudes of the moving breathing solitons are higher than those of the breathing solitons.

3.2. Quasi-breathing solitons

Now we consider the case of $\epsilon \neq 0$. In order to give an example of quasi-breathing solitons we take $\omega_0 = 0.4$, $\bar{\omega} = 2$ and $\epsilon = 0.1$ in (5), i.e. the ratio of the confining frequency $\omega = \sqrt{0.16 + 0.1 \cos(0.2t)}$ is a time-dependent function, which ensures that two linear independent solutions ξ_1 and ξ_2 of the Mathieu equation (5) belong to its stability region. So (5) has two incommensurable frequencies. In this way, the localized matter wave given by the solutions (11) exhibits quasi-periodic behaviors and interactions are still space- and time-dependent. Figure 4 shows an example of such quasi-periodic behavior. The first to the fourth columns describe the time evolution of the density and contour profiles of the one-order wave functions $\psi_1^{(1)}$, $\psi_{-1}^{(2)}$, $\psi_0^{(2)}$ and the total density distribution $|\psi_1^{(1)}|^2 + |\psi_{-1}^{(2)}|^2 + |\psi_0^{(2)}|^2$, respectively. Figure 4(e) describes the amplitude (red) and the width (blue) of the quasi-breathing solitons. It can be observed the nonlinear matter waves are space-localized

and quasi-periodic with respect to time and it can also be found that the amplitude and width of the nonlinear waves are quasi-periodic versus t .

3.3. Resonant solitons

Here, we still consider the case $\epsilon \neq 0$, i.e. the ratio of the confining frequency ω is time-dependent. In this case, we choose $\omega_0 = 0.44$, $\bar{\omega} = 32$ and $\epsilon = 0.003$ in the Mathieu equation (5), which ensures that two linear independent solutions ξ_1 and ξ_2 of (5) belong to its instability region. Thus, the localized matter waves given by the solutions (11) show that the behaviors and interactions of the resonant solitons are still space- and time-dependent. Figure 5 shows the evolution of the density and contour profiles for the resonant solitons. The first to fourth columns in figure 5 demonstrate the evolution of the density and contour profiles of the one-order wave functions $\psi_1^{(1)}$, $\psi_{-1}^{(2)}$, $\psi_0^{(2)}$, and $|\psi_1^{(1)}|^2 + |\psi_{-1}^{(2)}|^2 + |\psi_0^{(2)}|^2$, respectively. It can be observed the nonlinear matter waves are space-localized and time resonant. Figure 5(e) shows the amplitude and width versus time for the resonant solitons. It can be observed that the amplitude of the resonant solitons is low and their width is large at the beginning. After a while the amplitudes become higher but the widths become smaller. This phenomenon appears gradually as time passes. So this nonlinear matter wave demonstrates resonant soliton behavior. This resonant behavior arises from the cooperation of the spatiotemporal inhomogeneous interactions and the trapping potential.

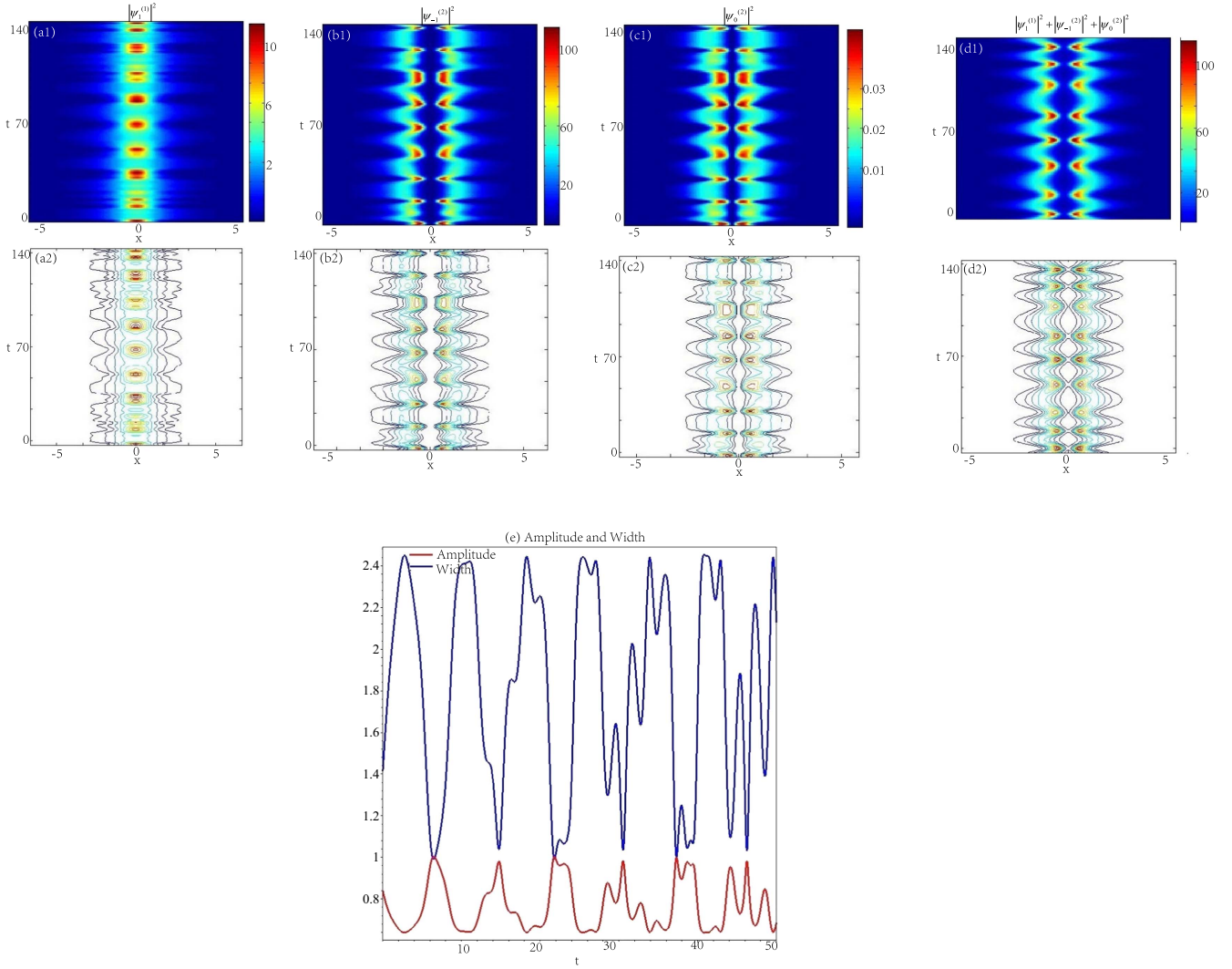


Figure 4. Dynamics of the quasi-breathing solitons in a spin-1 BEC with spatiotemporally modulated nonlinearities. Parts (a1) and (a2) show the evolution of the density and contour distribution $|\psi_1^{(1)}|^2$, respectively. Parts (b1) and (b2) show the evolution of the density and contour distribution $|\psi_{-1}^{(2)}|^2$, respectively. Parts (c1) and (c2) display the evolution of the density and contour distribution $|\psi_0^{(2)}|^2$, respectively. Parts (d1) and (d2) illustrate the evolution of the density and contour distribution $|\psi_1^{(1)}|^2 + |\psi_{-1}^{(2)}|^2 + |\psi_0^{(2)}|^2$, respectively. Part (e) illustrates the amplitude (red) and the width (blue). The ratio of the confining frequency is taken as $\omega = \sqrt{0.16 + 0.1\cos(0.2t)}$.

4. Stability analysis

Now we study the dynamical stability of the localized nonlinear wave solutions (11) by performing some numerical simulations. Here we run the numerical simulations using the split-step Fourier transformation. The domain is composed of $N = 512$ grid points and the step size of time integration is $\tau = 0.0001$. We take $\psi_j(x, 0)$ ($j = -1, 0, 1$) as the initial values and the simulations last up to $t = 200$. The simulation results show that:

- (a) when $\delta = 0$, the exact localized nonlinear wave solutions (11) are dynamically stable for $j = 1$ and $n = 0$, that is to say the one-order breathing soliton, quasi-breathing soliton and resonant soliton are all stable,

- (b) when $\delta \neq 0$, the moving solitons $\psi_1^{(1)}$ and $\psi_0^{(1)}$ are dynamically stable, while $\psi_{-1}^{(1)}$ is unstable.

Figure 6 shows the time evolution of the one-order breathing solitons $\psi_1^{(1)}$, $\psi_0^{(1)}$ and $\psi_{-1}^{(1)}$ for $\delta = 0$ and $\varepsilon = 0$ when the nonlinearities are taken as $g_n(x, t) = -g_s(x, t) = \frac{1}{8}\nu(t)^{-\frac{1}{2}}e^{-\frac{x^2}{\nu(t)}}$ and $\nu(t) = 5\sin\left(\frac{2}{5}t\right)^2 + 2\cos\left(\frac{2}{5}t\right)^2 + \sqrt{15}\sin\left(\frac{2}{5}t\right)\cos\left(\frac{2}{5}t\right)$, respectively. It can be observed that the one-order breathing solitons $\psi_1^{(1)}$, $\psi_0^{(1)}$ and $\psi_{-1}^{(1)}$ are dynamically stable.

Figure 7 shows the evolution of the one-order moving breathing solitons $\psi_1^{(1)}$, $\psi_0^{(1)}$ and $\psi_{-1}^{(1)}$ with $\delta = 1$, $\varepsilon = 0$ and $g_n(x, t) = -g_s(x, t) = \frac{1}{8}\nu(t)^{-\frac{1}{2}}e^{\left(1-\frac{x}{\nu(t)}\right)^2}$. It can be seen that the moving breathing solitons $\psi_1^{(1)}$ and $\psi_0^{(1)}$ are dynamically stable, while $\psi_{-1}^{(1)}$ is unstable.

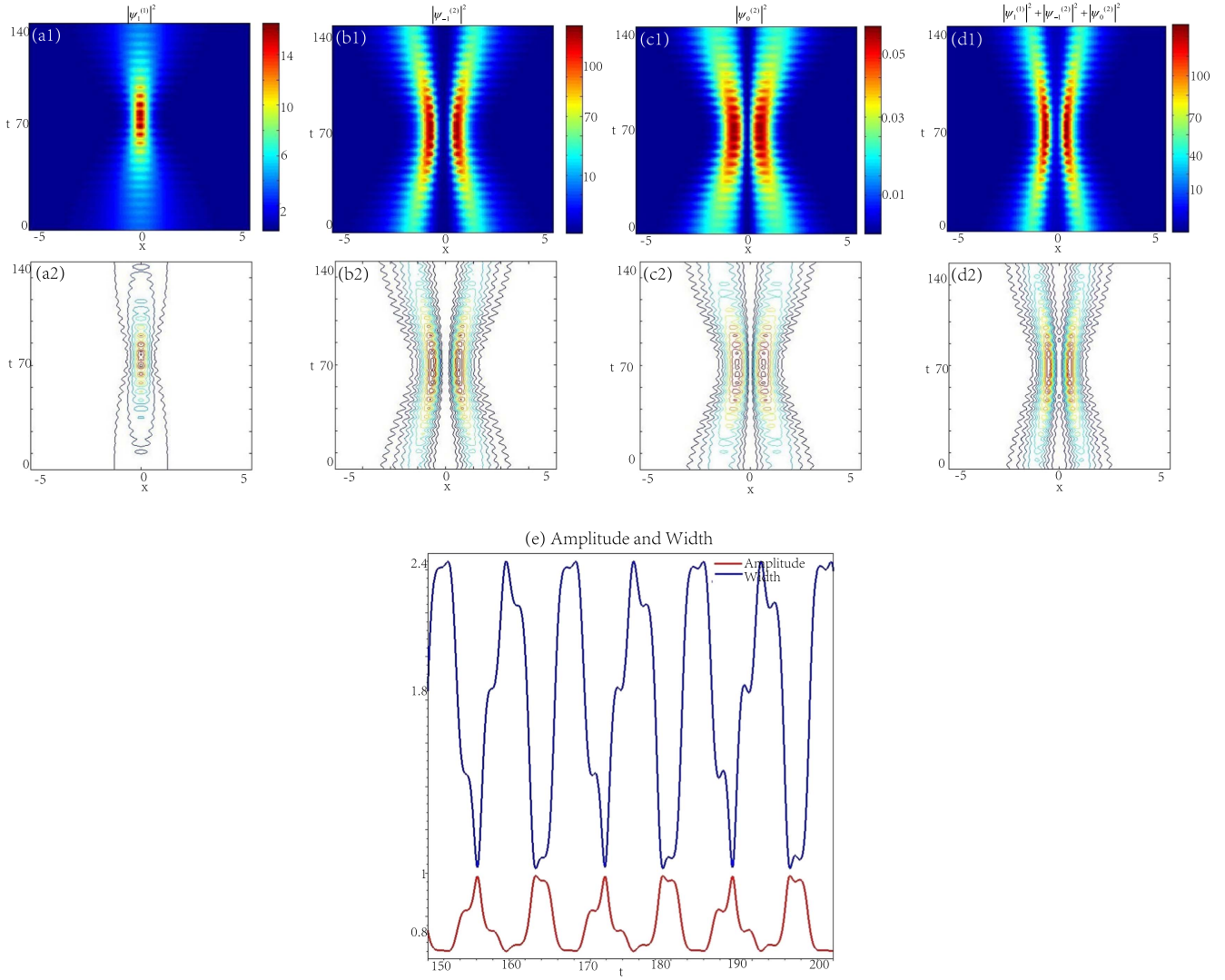


Figure 5. Dynamics of the resonant breathing solitons in a spin-1 BEC with spatiotemporally modulated nonlinearities. Parts (a1) and (a2) explain the evolution of the density and contour $|\psi_1|^2$, respectively. Parts (b1) and (b2) exhibit the evolution of the density and contour $|\psi_{-1}|^2$, respectively. Parts (c1) and (c2) show the evolution of the density and contour $|\psi_0|^2$, respectively. Parts (d1) and (d2) demonstrate the evolution of the density and contour $|\psi_1^{(1)}|^2 + |\psi_{-1}^{(2)}|^2 + |\psi_0^{(2)}|^2$, respectively. Parts (e) illustrates the amplitude of the breathing solitons (red) and the moving breathing solitons (blue). Here the ratio of the confining frequency $\omega = \sqrt{0.19 + 0.003\cos 32t}$.

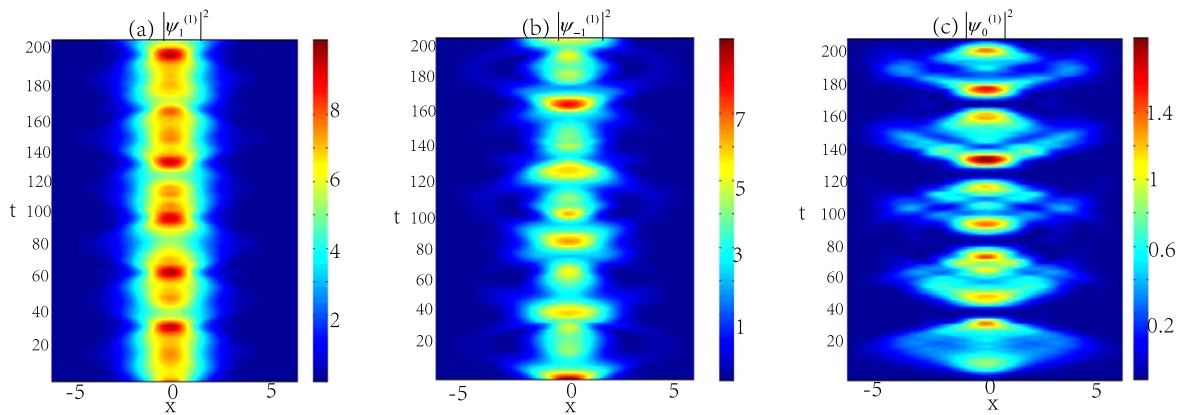


Figure 6. Evolution of the one-order breathing solitons for $\delta = 0$, $\varepsilon = 0$ and the nonlinearity $g_n(x, t) = -g_s(x, t) = \frac{1}{8}\nu(t)^{-\frac{1}{2}}e^{-\frac{x^2}{\nu(t)}}$. The other parameters are the same as used in figure 2.

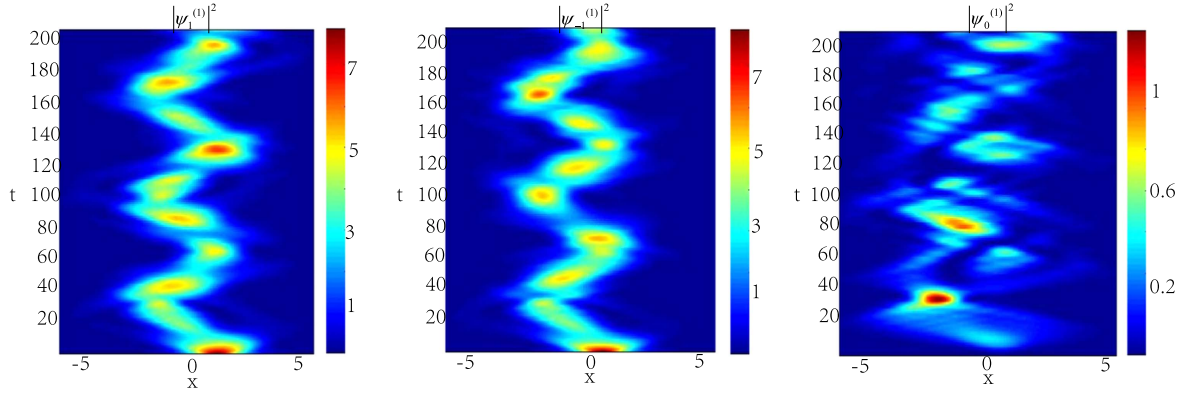


Figure 7. Evolution of the one-order moving breathing solitons with $\delta = 1$, $\varepsilon = 0$ and the nonlinearity $g_n(x, t) = -g_s(x, t) = \frac{1}{8}\nu(t)^{-\frac{1}{2}}e^{(1-\frac{x}{\nu(t)})^2}$. The other parameters are the same as used in figure 3.

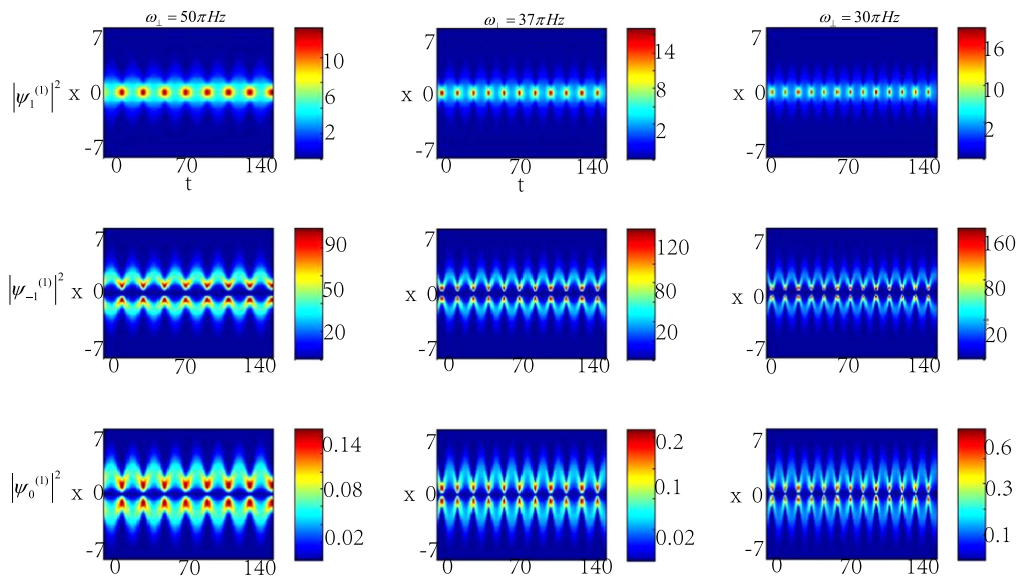


Figure 8. Impact of radial confinement on breathing solitons. The first to the third rows represent the time evolution of the density distributions $|\psi_1^{(1)}|^2$, $|\psi_{-1}^{(1)}|^2$ and $|\psi_0^{(1)}|^2$, respectively. The first column reveals the time evolution of the density distribution when $\omega_{\perp} = 50\pi$ Hz. The second column shows the time evolution of the density distribution when $\omega_{\perp} = 37\pi$ Hz. The third column shows the time evolution of the density distribution when $\omega_{\perp} = 30\pi$ Hz.

5. Conclusion and discussion

In this paper we have focused on the dynamics of spin-1 BECs with spatiotemporally dependent nonlinearities. Here, we take the sodium atom ^{23}Na ($N = 3 \times 10^6$) as an example to show how to create various soliton phenomena under the condition that the Zeeman energy E_j satisfies $E_1 + E_{-1} = E_0$. Breathing solitons can be observed when the interactions $g_n(x, t) = -g_s(x, t) = \frac{1}{8}\nu(t)^{-\frac{1}{2}}e^{-\frac{x^2}{\nu(t)}}$ are spatiotemporal nonlinearities and moving breathing solitons can be observed when the spatiotemporally modulated nonlinearities are $g_n(x, t) = -g_s(x, t) = \frac{1}{8}\nu(t)^{-\frac{1}{2}}e^{(1-\frac{x}{\nu(t)})^2}$ with confining frequencies in the transverse and axial directions of $\omega_x = 20\pi$ Hz and $\omega_{\perp} = 50\pi$ Hz, respectively. When the confining frequencies in the transverse direction are the

functions of t , quasi-breathing and resonant solitons may be observed. For example, when the nonlinearities are spatiotemporally modulated functions in the form of $g_n(x, t) = -g_s(x, t) = -e^{(\lambda(t)x + \delta(t))^2} / (8\lambda(t))$ with the confining frequencies $\omega_x = (16 + 3\cos 0.2t)\pi$ Hz and $\omega_{\perp} = 100\pi$ Hz, a quasi-breathing soliton can appear. A resonant soliton can appear with the confining frequencies $\omega_x = (19 + 0.03\cos 32t)\pi$ Hz and $\omega_{\perp} = 100\pi$ Hz. Based on the analytical expressions, we also discuss the impact of radial confinement on the soliton behaviors. It can be found that radial confinement ω_{\perp} can affect the period and amplitude of the solitons. We take breather solitons as an example to illustrate the impact of this in figure 8. Here, we take $\omega_{\perp} = 50\pi$ Hz, $\omega_{\perp} = 37\pi$ Hz and $\omega_{\perp} = 30\pi$ Hz separately. Figure 8 shows that the periods become smaller and the amplitude becomes larger with the decrease of radial

confinement ω_{\perp} . It should be pointed out that the present results are based the effective one-dimensional model in equations (1). As the equations include not only ω_x but also ω_{\perp} this allows some insight into the effect of radial trapping. It would be useful to make a rigorous investigation on a truly three-dimensional model in the future.

In summary, we have worked out the localized nonlinear matter wave solutions of the three-component GPEs with time- and space-dependent nonlinearities for $F = 1$ spinor BECs. These solutions are derived in terms of Jacobi elliptic functions and the Mathieu equation by similarity transformation. Further, we illustrate that the localization of the nonlinear matter wave takes the form of vector breathing solitons, moving breathing solitons, quasi-breathing solitons and resonant solitons. The dynamical stability of all types of vector solitons is analyzed by numerical stimulation. The results show that the one-order breathing solitons, quasi-breathing solitons, resonant soliton and moving breathing solitons apart from the matter wave ψ_0 are all stable. We hope that these dynamic behaviors of the spin-1 BECs with spatiotemporal nonlinearities can be realized in future experiments and help us to understand these phenomena further.

Acknowledgments

This work was supported by the NKRDP under grant no. 2016YFA0301500, the NSFC under grant nos 11434015, 61227902, 61378017 and KZ201610005011, the SKLQO-QOD under grant no. KF201403, the SPRPCAS under grant nos XDB01020300 and XDB21030300 and the Beijing Natural Science Foundation under grant no. 1182009.

ORCID iDs

Yu-Qin Yao  <https://orcid.org/0000-0003-4198-4459>

References

- [1] Pethick C J and Smith H 2002 *Bose–Einstein Condensation in Dilute Gases* (Cambridge: Cambridge University Press)
- [2] Ozeri R, Steinhäner N K J and Davidson N 2005 Colloquium: bulk Bogoliubov excitations in a Bose–Einstein condensate *Rev. Mod. Phys.* **77** 187
- [3] Ho T L and Shenoy V B 1996 Binary mixtures of Bose condensates of alkali atoms *Phys. Rev. Lett.* **77** 3276
Ho T L 1998 Spinor Bose condensates in optical traps *Phys. Rev. Lett.* **81** 742
- [4] Ohmi T and Machida K 1998 Bose–Einstein condensation with internal degrees of freedom in alkali atom gases *J. Phys. Soc. Japan* **67** 1822
Isoshima T, Machida K and Ohmi T 1998 Spin-domain formation in spinor Bose–Einstein condensation *Phys. Rev. A* **60** 4857
- [5] Stamper-Kurn D M et al 1998 Optical confinement of a Bose–Einstein condensate *Phys. Rev. Lett.* **80** 2027
- [6] Stenger J et al 1998 Spin domains in ground-state Bose–Einstein condensates *Nature* **396** 345
- [7] Vengalattore M, Leslie S R, Guzman J and Stamper-Kurn D M 2008 Spontaneously modulated spin textures in a dipolar spinor Bose–Einstein condensate *Phys. Rev. Lett.* **100** 170403
- [8] Kanna T, Mareswaran R B and Sakkaravarthi K 2014 Non-autonomous bright matter wave solitons in spinor Bose–Einstein condensates *Phys. Rev. A* **378** 158
- [9] Liu Y K and Yang S J 2014 Exact solitons and manifold mixing dynamics in the spin-orbit-coupled spinor condensates *EPL* **108** 30004
- [10] Seo S W, Kang S, Kwon W J and Shin Y I 2015 Half-quantum vortices in an antiferromagnetic spinor Bose–Einstein condensate *Phys. Rev. Lett.* **115** 015301
- [11] Seo S W, Kang S, Kwon W J and Shin Y I 2016 Collisional dynamics of half-quantum vortices in a spinor Bose–Einstein condensate *Phys. Rev. Lett.* **116** 85301
- [12] Oshima T and Kawaguchi Y 2016 Spin Hall effect in a spinor dipolar Bose–Einstein condensate *Phys. Rev. A* **93** 053605
- [13] Ollikainen T, Masuda S, Mottonen M and Nakahara M 2017 Counterdiabatic vortex pump in spinor Bose–Einstein condensates *Phys. Rev. A* **95** 013615
- [14] Borgh M O, Lovegrove J and Ruostekoski J 2017 Internal structure and stability of vortices in a dipolar spinor Bose–Einstein condensate *Phys. Rev. A* **95** 053601
- [15] Gautam S and Adhikari S K 2017 Vortex-bright solitons in a spin-orbit-coupled spin-1 condensate *Phys. Rev. A* **91** 013608
- [16] Dutton Z, Budde M, Slowe C and Hau L V 2001 Observation of quantum shock waves created with ultra-compressed slow light pulses in a Bose–Einstein condensate *Science* **293** 663
- [17] Strecker K E, Partridge G B, Truscott A G and Hulet R G 2002 Formation and propagation of matter-wave soliton trains *Nature* **417** 150
- [18] Kengne E and Talla P K 2006 Dynamics of bright matter wave solitons in Bose–Einstein condensates in an expulsive parabolic and complex potential *J. Phys. B* **39** 3679
- [19] Sekh G A, Pepe F V, Facchi P, Pascazio S and Salerno M 2015 Split and overlapped binary solitons in optical lattices *Phys. Rev. A* **92** 013639
- [20] Meystre P 2001 *Atom Optics (Springer Series on Atomic, Optical, and Plasma Physics 33)* (New York: Springer) 249–68
- [21] Chin C, Grimm R, Julienne P and Tiesinga E 2010 Feshbach resonances in ultracold gases *Rev. Mod. Phys.* **82** 1225
- [22] Bloch I, Dalibard J and Zwerger W 2008 Many-body physics with ultracold gases *Rev. Mod. Phys.* **80** 885
- [23] Kengne E, Shehou A and Lakhssassi A 2016 Dynamics of matter-wave solitons in Bose–Einstein condensates with time-dependent scattering length and complex potentials *Eur. Phys. J. B* **89** 78
Abdullaev F K, Caputo J G, Kraenkel R A and Malomed B A 2003 Controlling collapse in Bose–Einstein condensates by temporal modulation of the scattering length *Phys. Rev. A* **67** 013605
- [24] Radha R, Kumar V R and Porsezian K 2008 Remote controlling the dynamics of Bose–Einstein condensates through time-dependent atomic feeding and trap *J. Phys. A: Math. Theor.* **41** 315209
- [25] Wang D S, Hu X H and Liu W M 2010 Quantized quasi-two-dimensional Bose–Einstein condensates with spatially modulated nonlinearity *Phys. Rev. A* **82** 023612
Liang Z X, Zhang Z D and Liu W M 2005 Dynamics of a bright soliton in Bose–Einstein condensates with time-dependent atomic scattering length in an expulsive parabolic potential *Phys. Rev. Lett.* **94** 050402
- [26] Alexander T J, Heenan K, Salerno M and Ostrovskaya E A 2012 Dynamics of matter-wave solitons in harmonic traps with flashing optical lattices *Phys. Rev. A* **85** 063626
Yao Y Q, Li J, Han W and Liu W M 2016 Localized spatially

- nonlinear matter waves in atomic-molecular Bose–Einstein condensates with space-modulated nonlinearity *Sci. Rep.* **89** 78
- Burlak G and Malomed B A 2008 Dynamics of matter-wave solitons in a time-modulated two-dimensional optical lattice *Phys. Rev. A* **77** 053606
- [27] Zhang J F, Li Y S, Meng J P, Wu L and Malomed B A 2010 Matter-wave solitons and finite-amplitude Bloch waves in optical lattices with spatially modulated nonlinearity *Phys. Rev. A* **82** 033614
- [28] Tiesinga E, Verhaar B J and Stoof H T C 1993 Threshold and resonance phenomena in ultracold ground-state collisions *Phys. Rev. A* **47** 4114
- [29] Inoué S, Andrews M R, Stenger J, Miesner H-J, Stamper-Kurn D M and Ketterle W 1998 Observation of Feshbach resonances in a Bose–Einstein condensate *Nature* **392** 151–4
- [30] Fedichev P, Kagan Y, Shlyapnikov G V and Walraven J T M 1996 Influence of nearly resonant light on the scattering length in low-temperature atomic gases *Phys. Rev. Lett.* **77** 2913
- [31] Theis M, Thalhammer G, Winkler K, Hellwig M, Ruff G, Grimm R and Hecker Denschlag J 2004 Tuning the scattering length with an optically induced Feshbach resonance *Phys. Rev. Lett.* **93** 123001
- [32] Olshanii M 1998 Atomic scattering in the presence of an external confinement and a gas of impenetrable bosons *Phys. Rev. Lett.* **81** 938
- [33] Haller E *et al* 2009 Realization of an excited, strongly correlated quantum gas phase *Science* **325** 1224
- [34] Zhang R, Cheng Y T, Zhai H and Zhang P 2015 Orbital Feshbach resonance in alkali-earth atoms *Phys. Rev. Lett.* **115** 135301
- [35] Pagano G, Mancini M, Cappellini G, Livi L, Sias C, Catani J, Inguscio M and Fallani L 2015 Strongly interacting gas of two-electron fermions at an orbital Feshbach resonance *Phys. Rev. Lett.* **115** 265301
- [36] Yamazaki R, Taie S, Sugawa S and Takahashi Y 2010 Submicron spatial modulation of an interatomic interaction in a Bose–Einstein condensate *Phys. Rev. Lett.* **105** 050405
- [37] Qi R and Zhai H 2011 Bound states and scattering resonances induced by spatially modulated interactions *Phys. Rev. Lett.* **106** 163201
- [38] Claussen N R, Donley E A, Thompson S T and Wieman C E 2002 Microscopic dynamics in a strongly interacting Bose–Einstein condensate *Phys. Rev. Lett.* **89** 010401
- [39] Kevrekidis P G, Theocharis G, Frantzeskakis D J and Malomed B A 2003 Feshbach resonance management for Bose–Einstein condensates *Phys. Rev. Lett.* **90** 230401
- [40] Strecker K E, Partridge G B, Truscott A G and Hulet R G 2002 Formation and propagation of matter-wave soliton trains *Nature* **417** 150
- [41] Greiner M, Regal C A and Jin D S 2005 Probing the excitation spectrum of a Fermi gas in the BCS–BEC crossover regime *Phys. Rev. Lett.* **94** 070403
- [42] Clark L W, Ha L-C, Xu C-Y and Chin C 2015 Quantum dynamics with spatiotemporal control of interactions in a stable Bose–Einstein condensate *Phys. Rev. Lett.* **115** 155301
- [43] Gerton J M, Frew B J and Hulet R G 2001 Photoassociative frequency shift in a quantum degenerate gas *Phys. Rev. A* **64** 053410
- [44] Bergeman T, Moore M G and Olshanii M 2003 Atom–atom scattering under cylindrical harmonic confinement: numerical and analytic studies of the confinement induced resonance *Phys. Rev. Lett.* **91** 163201
- [45] Lamporesi G, Donadello S, Serafini S and Ferrari G 2013 Compact high-flux source of cold sodium atoms *Rev. Sci. Instrum.* **84** 063102
- [46] Law C K, Pu H and Bigelow N P 1998 Quantum spins mixing in spinor Bose–Einstein condensates *Phys. Rev. Lett.* **81** 5257
- [47] Madison K W, Chevy F, Bretin V and Dalibard J 2001 Stationary states of a rotating Bose–Einstein condensate: routes to vortex nucleation *Phys. Rev. Lett.* **86** 4443
- [48] Klausen N N, Bohn J L and Greene C H 2001 Nature of spinor Bose–Einstein condensates in rubidium *Phys. Rev. A* **64** 053602
- [49] Dabrowska-Wüster B J, Ostrovskaya E A, Alexander T J and Kivshar Y S 2007 Multicomponent gap solitons in spinor Bose–Einstein condensates *Phys. Rev. A* **75** 023617
- [50] Nicolin A I 2011 Resonant wave formation in Bose–Einstein condensates *Phys. Rev. E* **84** 056202
- [51] Raportaru M C 2012 Formation of Faraday and resonant waves in driven Bose–Einstein condensates *Rom. Rep. Phys.* **64** 105